

On Topology-based Cohesive Interface Element Insertion along Periodic Boundary Surfaces

Sunday Aduloloju ^a, Timothy J. Truster ^a †

^a Department of Civil and Environmental Engineering, University of Tennessee, Knoxville, 318 John D. Tickle Engineering Building, Knoxville, TN 37996

Engineering Fracture Mechanics

Abstract

This paper extends the discontinuous element insertion program (DEIP) to insert cohesive interface elements along periodic surfaces of representative volume elements (RVE). The key enabler involves zipping the RVE mesh along its periodic surfaces, generating a topologically closed grid similar to a torus. Such models are relevant to modeling grain boundary sliding and cracking in polycrystalline materials, for which a two-dimensional example is provided with hexagonal-shaped grains.

Key Words: Interface elements, couplers, periodic boundary surfaces, mesh zipping

1. Introduction

Micromechanical modeling is becoming increasingly popular as a robust and computationally efficient predictive tool for the accurate modeling of nonlinear response at grain boundaries of metallic alloys. This method is also being applied to model deformation and fracture in engineered materials such as composites and metamaterials. The accurate definition of the representative volume element (RVE) and the construction of the micro scale boundary value problem are essential to determining the local behavior across the macroscale [1]. Particularly, the analysis of damage or sliding along interface within RVE having periodic boundary conditions requires the generation of periodic finite element meshes that enable discontinuities in the solution fields at the periodic surfaces to avoid inserting the boundary layer differently than the interior.

The ability to model complex RVE in higher dimensions facilitates the study of several deformation modes, such as uniaxial, plane strain, shear deformation, and even arbitrary principal stress states [2]. The modeling of interfacial phenomena under these conditions is typically accomplished using interface elements, such as cohesive zone (CZ) models [3, 4]. Unfortunately, mesh generators have only been able to insert interface elements into the RVE mesh within the interior but excluding the treatment of grain boundaries along the RVE periodic surfaces because the treatment of nodal constraints for the periodic conditions at the surfaces in 2 and 3 dimensions

† Assistant Professor. Corresponding author: Ph: (865) 974-1913; Fax: (865) 974-2669, e-mail: ttruster@utk.edu

37 may be non-trivial. Thus, we describe the extension of the zero-thickness interface element
38 insertion algorithm [5, 6] for producing the FE meshes required for modeling interface damage [7,
39 8] to include cohesive element (termed herein as “couplers”) insertion at the boundary surfaces to
40 allow for periodic boundary modeling of complex 2D and 3D RVE problems. A 2-dimensional
41 example of RVE grain boundary sliding and opening in a polycrystalline periodic structure
42 demonstrates the algorithm’s capabilities.

43 **2. Truly Periodic Boundary Model**

44 Many existing works [1, 3, 4] represent the RVE using a block or cuboid domain since this shape
45 is simple to create, the periodic conditions along the planar cube faces are easy to describe, and
46 the multipoint constraints are easy to generate. However, the truly periodic model is the direct
47 instantiation of the microstructure without artificial planar cuts, and then arbitrary macroscale
48 loading conditions can be imposed. For interfacial sliding and cracking in a block domain, couplers
49 are inserted only along the interior grain boundaries because of the artificial cuts. On the other
50 hand, the couplers are inserted along all grain boundaries for the truly periodic model to allow for
51 sliding and opening at the periodic interfaces. In the block RVE model, the artificial cuts could
52 cause artificial stress concentrations, and the interior grain boundaries terminating on the RVE
53 surface are restricted against sliding outward. Therefore, a more sophisticated coupler insertion
54 algorithm is required.

55 **3. Coupler Insertion Algorithm**

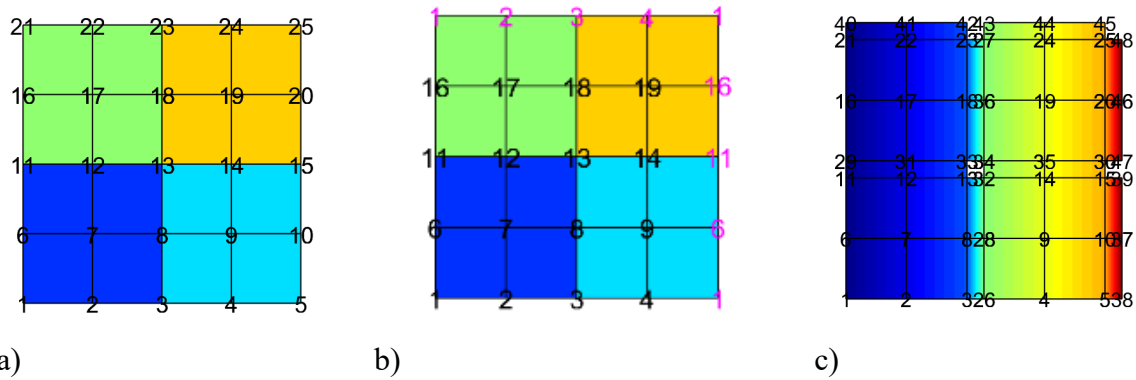
56 The algorithm described herein performs topologically based coupler insertion into conforming
57 FE meshes to generate suitable meshes for periodic boundary analysis. The required input data are
58 the spatial nodal coordinates, the element connectivity array, the elements contained in each region,
59 the list of the nodal multipoint constraints for periodicity, and a flag to insert couplers in regions
60 and/or region boundaries. The algorithm then inserts the couplers at the element boundaries
61 belonging to the sets along interior interfaces and periodic surfaces of the interface and periodic
62 boundary. Note that these periodic conditions are expressed through nodal constraints of the form:

$$\mathbf{u}^+ - \mathbf{u}^- = \varepsilon(\mathbf{x}^+ - \mathbf{x}^-) \quad (1)$$

63 where \mathbf{x} is the spatial coordinate, \mathbf{u} is the displacement, ε is the macroscopic strain, and $+$
64 and $-$ refer to the opposite sides of paired surfaces on the RVE boundary.

65 The key idea for coupler insertion at the periodic surfaces is the creation of a topologically-closed
66 mesh analogous to a torus by forcing shared facets between pairs of opposing opposite boundaries.
67 The key new steps are the zipping of the mesh and the renumbering of the nodes followed by
68 element connectivity update of the mesh. This process is automated using the multipoint constraint
69 list, collapsing linked nodes into a single instance, creating a mesh with only element interfaces
70 and no boundary surfaces. Then the existing algorithm from [5, 6] is executed with minimal
71 modifications to produce the new nodes, couplers and periodicity links.

72 These additional steps are outlined for an example 2D mesh of 16 elements, 25 nodes and 4 regions
73 denoted by different colors in Figure 1 (a). The automated process for determining which sets of
74 couplers to insert and nodes to duplicate for periodic finite element domains consists of seven
75 phases. In the first phase, the periodic boundary condition node links are employed to renumber
76 connected nodes with a single identifier. For example, the four boundary nodes 1, 5, 21, and 25
77 are linked and all set to 1. The connectivity array of nodes attached to elements is then updated
78 with this renumbering as shown in Figure 1 (b). Essentially, this zips the mesh together, so that the
79 upper right yellow element is adjacent to the upper left green element, and so forth. The next five
80 phases proceed on this modified connectivity and are identical to the original algorithm described
81 in [5] and the associated user manual. These phases identify all the element interface facets of the
82 mesh and duplicate the nodes along the region boundaries designated for coupler, by the user. The
83 final phase extends the sixth phase of [5] to generate the coupler connectivity as well as the new
84 set of periodic boundary condition node links.



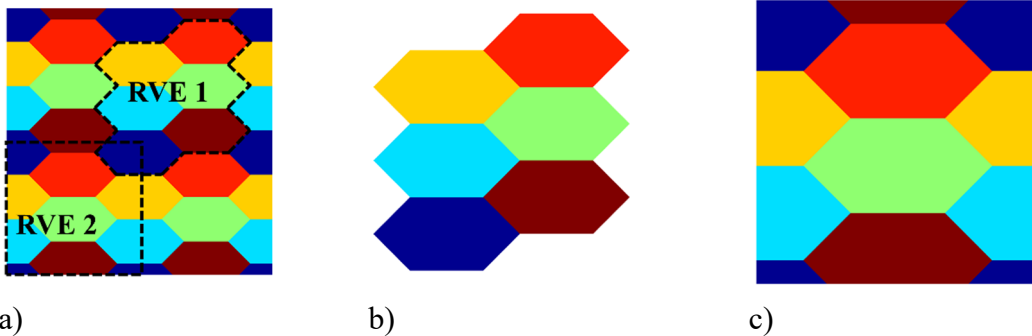
85 Figure 1. Square finite element mesh containing 4 regions: (a) initial mesh; (b) node numbering
86 for zipped mesh; (c) mesh after coupler insertion along interfaces and periodic surfaces.

87 The unzipped finite element mesh produced after coupler insertion is shown in Figure 1 (c) with
88 the interfaces and couplers expanded for clarity. When a coupler is inserted along the RVE surface
89 (which is known from phase 1 and 3), extra copies of the attached nodes are generated. For
90 example, the coupler on the right of the domain is connected to nodes 5, 10, 37, and 38; node links
91 then attach node 38 to node 1 and node 37 to node 6 on the left boundary of the domain. Thus
92 nodes 1 and 6 are the – side and nodes 37 and 38 become the + side in constraint (1). Caution
93 is exercised by using the region number to ensure that all couplers are inserted along the same side
94 of the shared interface. Also, linearly dependent periodicity constants are removed by converting
95 the link equations to row-echelon form.

96 Thus the enhancements of the original DEIP program presented in [5, 6] is the creation of FE
97 meshes required for solving periodic boundary conditions and insertion of cohesive couplers at the
98 periodic boundary to allow for interface sliding and cracking in truly periodic models.

99 **4. Two Dimensional Example**

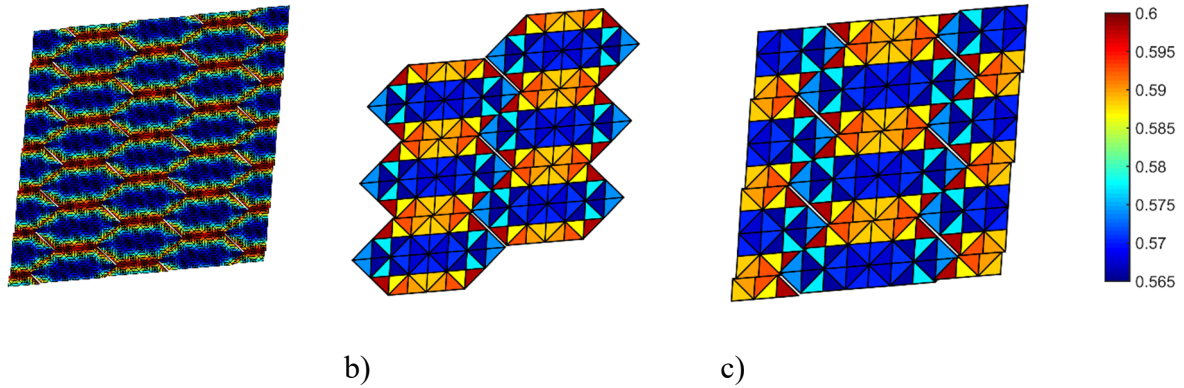
100 As a verification example of the node duplication algorithm, a patch test was performed on a
 101 periodic polycrystalline domain containing hexagonal grains. Due to the repeating geometrical
 102 structures, several different “windows” can be chosen to form an RVE, and in fact each should
 103 produce identical bulk response if each grain has identical properties. Hence, we select RVE1 as a
 104 truly periodic model with grain boundaries (and couplers) on the periodic surfaces, while RVE2 is
 105 a block model chosen such that no grain boundaries lie on the block surface. The solid meshes
 106 contain 288 constant strain triangular (T3) elements in the coarsest possible uniform arrangement
 107 for a total of 167 nodes in RVE1 and 169 nodes in RVE2 as shown in Figure 2 (b) and (c). A
 108 macroscopic shear strain $\gamma_{xy} = 0.02$ was applied to both RVEs, and the solid elements employ
 109 linear elasticity with $E = 100 \text{ MPa}$ and $\nu = 0.25$. The interfaces were modeled as linear elastic
 110 cohesive elements, and the periodic boundary conditions were enforced as node pairs constrained
 111 together with two “master nodes” via Lagrange multiplier, similar to [2]. For a very high cohesive
 112 stiffness of $500 \times 10^{10} \text{ N/mm}^3$, a constant shear stress of 0.8 MPa throughout the grains was
 113 computed by the model, thereby satisfying the patch test.



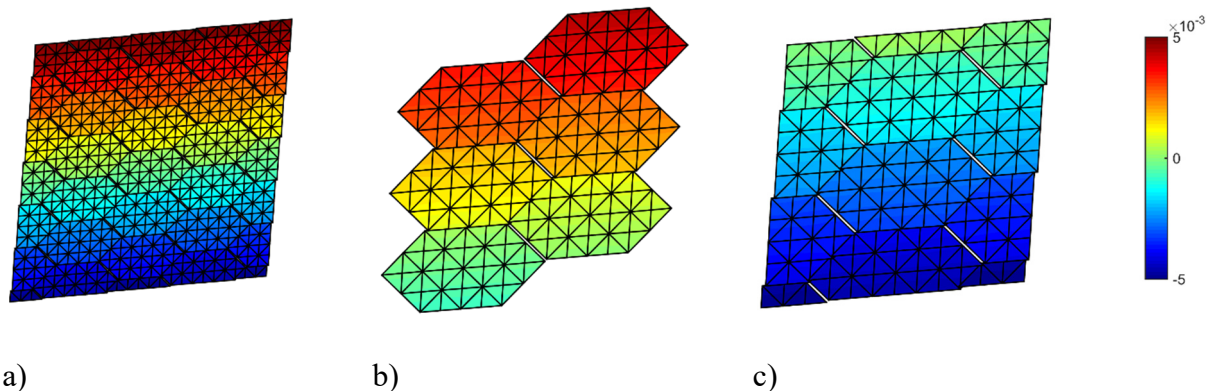
114 Figure 2. Periodic polycrystalline domain: (a) overall microstructure; (b) truly periodic RVE1;
 115 (c) block RVE2

116 The solution on a very fine mesh for a lower cohesive stiffness of 500 N/mm^3 is shown in Figure
 117 3 (a). The stress is slightly greater along horizontal interfaces than on inclined interfaces of the
 118 grains by examining Figure 3 (a) – (c). The computed elemental stresses for RVE1 and RVE2 are
 119 in perfect agreement spatially and also share features with the refined model. We also observe
 120 relative horizontal sliding of the grains and separation along the diagonal interfaces. Next, the
 121 displacement u_x contour plots in Figure 4 (b) and (c) correspond with the location of the RVEs
 122 within the larger instantiation of the polycrystalline microstructure in Figure 4 (a). Thus, these
 123 results confirm that the choice of the RVE windows does not change the effective microscale
 124 response so long as the cohesive interfaces are properly accounted for. These examples in Sections

125 3 and 4 as well as others in three dimensions are provided within an open-source MATLAB[©]
126 version of the code at <https://bitbucket.org/trusterresearchgroup/deiprogram>.
127



128 Figure 3. Stress σ_{xy} contour: (a) refined mesh of overall microstructure; (b) RVE1; (c) RVE2



129 Figure 4. Displacement u_x contour: (a) coarse overall mesh; (b) RVE1; (c) RVE2

130 5. Conclusion

131 The proposed topologically-based algorithm enables cohesive interface element insertion along
132 periodic boundary surfaces in two and three dimensions. It builds seamlessly onto an existing
133 method by introducing the automatic generation of a topologically-closed mesh analogous to a
134 torus. Results from a periodic polycrystalline domain with hexagonal grains and interfaces
135 allowing sliding and opening verify that the insertion algorithm generates the proper node
136 duplication and interface elements on different yet mechanically equivalent RVEs.

137 Acknowledgements

138 This material is based upon work supported by the National Science Foundation under Grant No.
139 CMMI-1641054.

140 **References**

141 1. Geers, M.G., V.G. Kouznetsova, and W. Brekelmans, *Multi-scale computational*
142 *homogenization: Trends and challenges*. Journal of Computational and Applied
143 Mathematics, 2010. **234**(7): p. 2175-2182.

144 2. Danielsson, M., D. Parks, and M. Boyce, *Three-dimensional micromechanical modeling of*
145 *voided polymeric materials*. Journal of the Mechanics and Physics of Solids, 2002. **50**(2):
146 p. 351-379.

147 3. Benedetti, I. and M. Aliabadi, *A three-dimensional cohesive-frictional grain-boundary*
148 *micromechanical model for intergranular degradation and failure in polycrystalline*
149 *materials*. Computer Methods in Applied Mechanics and Engineering, 2013. **265**: p. 36-62.

150 4. Espinosa, H.D. and P.D. Zavattieri, *A grain level model for the study of failure initiation*
151 *and evolution in polycrystalline brittle materials. Part I: Theory and numerical*
152 *implementation*. Mechanics of Materials, 2003. **35**(3-6): p. 333-364.

153 5. Truster, T.J., *DEIP, discontinuous element insertion Program—Mesh generation for*
154 *interfacial finite element modeling*. SoftwareX, 2018. **7**: p. 162-170.

155 6. Truster, T.J., *On interface element insertion into three-dimensional meshes*. Engineering
156 Fracture Mechanics, 2016. **153**: p. 171-174.

157 7. Truster, T.J. and A. Masud, *A discontinuous/continuous Galerkin method for modeling of*
158 *interphase damage in fibrous composite systems*. Computational Mechanics, 2013. **52**(3):
159 p. 499-514.

160 8. Aduloju, S.C. and T.J. Truster, *A variational multiscale discontinuous Galerkin*
161 *formulation for both implicit and explicit dynamic modeling of interfacial fracture*.
162 Computer Methods in Applied Mechanics and Engineering, 2019. **343**: p. 602-630.

163